The thermal coupling enhancement thresholds apparent in Figs. 1 and 2 are compared in Table 1 to the corresponding thresholds for the formation of surface plasmas, taken from Ref. 4. There the plasma thresholds were measured for the same four metals and with the same laser, but with an effective beam spot diameter of 0.94 cm. The plasma thresholds listed in column 1 of Table 1 are the incident pulse fluence levels for which surface plasma ignition occurs halfway through the laser pulse. The largest observed coupling coefficients α_{max} and the constant energy deposited E_a are also tabulated. In Table 1 the material-dependent thermal coupling enhancement thresholds are clearly correlated with the material-dependent plasma formation thresholds. The lower thresholds (titanium and stainless steel) are associated with the higher values of α_{max} and the higher values of constant deposited energy $E_a = \alpha E_i$.

The variation of total thermal coupling to aluminum with ambient target pressure was measured for laser pulses of about 130 J. For air environment the coefficient α increased smoothly from 0.05 to 0.08 as pressure was reduced from 1 to 10^{-3} atm. The trend of decreasing α with increasing pressure is associated with the increasing density and shielding effect of the surface plasmas at higher ambient pressures.

Large differences in measured thermal coupling for cases of similar total incident fluences have been attributed to differences in the shape of the laser pulse time profile.[11] To investigate this effect, measured coupling coefficients were compared for pulse lengths 4 and 7 μs FWHM for both aluminum and titanium. There was no major shift in the thresholds due to this change of pulse length. The data above threshold were least-squares fitted to the power law $\alpha = aE_i^{-b}$. Short-pulse values of b were near unity for both metals in agreement with the overall E^{-1} dependence noted above. The long-pulse exponents of incident energy, $b = 0.84$ for aluminum and 0.70 for titanium, indicate that for the present conditions the long-pulse absolute energy deposited in the target continues to increase with incident energy even well above the plasma threshold.

Discussion

Two previous measurements of total coupling to aluminum at other wavelengths are notable because of the large focal spots used. Measurements at 1.06 μm by Hettche et al.[6] show a maximum $\alpha = 0.22$ for spot diameter of 0.56 cm ($\hat{\tau} \sim 7$). At 10.6 μm Marcus et al.[1] obtained values of α up to 0.33 on mechanically abraded targets for a spot diameter of 2.8 cm ($\hat{\tau} = 5.4$).

Certain reservations apply to all large-$\hat{\tau}$ measurement of total coupling. The radial spreading of the surface plasma can give contributions to the total coupling via target heating outside the beam spot.[12] This effect is minimized by minimizing $\hat{\tau}$, but the one-dimensional coupling, which is expected to scale to larger-spot conditions, is better indicated by spot-center measurements of local coupling $\alpha_r(0)$, which are insensitive to edge effects.

It should be noted, however, that the condition $\hat{\tau} \sim 1$ is not in itself sufficient to insure the "practical significance" of a thermal coupling measurement. Thermal effects depend on the energy fluence coupled to the target

$$e_a(r) = \alpha_r(r)\, e_i(r) = \alpha_r(r)\, q_i^{ave} t_p \qquad (1)$$

where q_i^{ave} is an average incident irradiance. An optimized $\alpha_r(r)$ can be maintained at $\hat{\tau} = ct_p/r_b = 1$ by making t_p very short, but the useful e_a then approaches zero due to the small $e_i(r)$ in Eq. (1). A rough lower limit for a "useful" t_p may be set by using $\alpha_r(r) \lesssim 0.2$ and a usable $q_i^{ave} \lesssim 10^8$ W/cm^2 (due to axial decoupling as well as propagation limitations) to give the requirement $t_p \gtrsim 10^{-7}$ s.

Finally, the common assumption that $\hat{\tau} = 1$ is optimum should be used with care. If we minimize the incident pulse energy E_i required to deliver a specified absorbed fluence $e_a(r)$, several recent semi-empirical models of coupling data yield $2 < \hat{\tau} < 3$; that of Hall[13] gives $\hat{\tau} = 2.7$.

Acknowledgment

This work was supported by the U.S. Air Force Weapons Laboratory, Kirtland Air Force Base, New Mex., under Contract F29601-76-C-0030. The authors are indebted to L.A. Alexander Jr. for technical assistance.

References

[1] Marcus, S., Lowder, J.E., and Mooney, D.L., "Large-spot Thermal Coupling of CO_2 Laser Radiation to Metallic Surfaces," *Journal of Applied Physics,* Vol. 47, July 1976, pp. 2966-2968.

[2] Ferriter, N., Maiden, D.E., Winslow, A.M., and Fleck, J.A., "Laser-Beam Optimization for Momentum Transfer by Laser-Supported Detonation Waves," *AIAA Journal,* Vol. 15, Nov. 1977, pp. 1597-1603.

[3] Robin, J.E. and Nordin, P., "Effects of Gravitationally-Induced Melt Removal on CW Laser Melt-Through of Opaque Solids," *Applied Physics Letters,* Vol. 27, Dec. 1975, pp. 593-595.

[4] Nichols, D.B. and Hall, R.B., "Threshold Conditions for the Formation of Surface Plasmas by HF and DF Laser Radiation," *Journal of Applied Physics,* Vol. 49, Oct. 1978, pp. 5155-5164.

[5] Wei, P.S.P. and Nichols, D.B., "Spectroscopic Diagnostics of Laser-Supported Absorption (LSA) Waves Produced by a HF Laser," *Journal of Applied Physics,* Vol. 47, July 1976, pp. 3054-3056.

[6] Hettche, L.R., Tucker, T.R., Schriempf, J.T., Stegman, R.L., and Metz, S.A., "Mechanical Response and Thermal Coupling of Metallic Targets to High-Intensity 1.06-μ Laser Radiation," *Journal of Applied Physics,* Vol. 47, April 1976, pp. 1415-1421.

[7] Pirri, A.N., Root, R.G., and Wu, P.K.S., "Plasma Energy Transfer to Metal Surfaces Irradiated by Pulsed Lasers," *AIAA Journal,* Vol. 16, Sept. 1978, pp. 1296-1304.

[8] Boni, A.A., Su, F.Y., Thomas, P.D., and Musal, H.M., "Theoretical Study of Laser-Target Interactions," Science Applications Inc., LaJolla, Calif., SAI 77-567LJ, May 1977.

[9] Nichols, D.B., Hall, R.B., and McClure, J.D., "Photoinitiated $F_2 + H_2/D_2$ Chain-Reaction Laser with High Electrical Efficiency," *Journal of Applied Physics,* Vol. 47, Sept. 1976, pp. 4026-4030.

[10] Pond, C.R., Hall R.B., and Nichols, D.B., "HF Laser Spectral Analysis Using Near-Field Holography," *Applied Optics,* Vol. 16, Jan. 1977, pp. 67-69.

[11] Manlief, S.K., Mooney, D.L., and Marcus, S., "Repetitively Pulsed CO_2 Laser-Target Interaction," MIT Lincoln Laboratory, Lexington, Mass., LTP-34, Aug. 1976.

[12] Hall, R.B., Maher, W.E., Nelson, D.J., and Nichols, D.B., "High Power Laser Coupling," USAF Rept. AFWL-TR-77-34, 1977, pp. 78-81.

[13] Maher, W.E., Nichols, D.B., and Hall, R.B., "Three-dimensional Plasma Effects on Enhanced Thermal Coupling of Laser Beams," IEEE Conference on Plasma Science, Quebec, Canada, June 1979.

Shock Tunnel Measurement of Ionization Rates in Hydrogen

R.J. Stalker*
University of Queensland, Australia

SIGNIFICANT nonequilibrium ionization may occur during atmospheric entry of probes to the outer planets,[1] and therefore knowledge of the rate of thermal ionization of

Received May 9, 1979; revision received Sept. 4, 1979.

Index categories: Thermochemistry and Chemical Kinetics; Reactive Flows; Entry Vehicle Testing, Flight and Ground.

*Professor, Dept. of Mechanical Engineering. Member AIAA.

Table 1 Rate constants[1,3]

Reaction	Forward rate constant (cm^3 $mole^{-1}$ s^{-1}) A	B
$H+e=H^*+e$ $H^*+e=H^++2e$	$2.8\times10^{14}\sqrt{T_e}\ \exp(-10/kT_e)$	$4.1\times10^{13}\sqrt{T_e}\ \exp(-10/kT_e)$
$H+H=H^*+H$ $H^*+H=H^++e+H$	$4.9\times10^{11}\sqrt{T}\ \exp(-10/kT)$	$6.2\times10^{10}\sqrt{T}\ \exp(-10/kT)$
$H+He=H^*+He$ $H^*+He=H^++e+He$	$4.9\times10^{11}\sqrt{T}\ \exp(-10/kT)$	$6.2\times10^{10}\sqrt{T}\ \exp(-10/kT)$

hydrogen is required for analysis of entry body flowfields. Initial measurements were made by Belozerov and Measures,[2] but the values obtained were later reduced by Leibowitz[3] through shock tube measurements of radiative relaxation in a 0.21 H_2 – 0.79 He mixture. He obtained the set of rate constants for the dominant rate determining processes shown under A in Table 1. Subsequently, Leibowitz and Kuo[1] reported further measurements at higher shock speeds, with a 0.85 H_2 – 0.15 He mixture, which led them to adopt the rate constants shown under B in Table 1. It can be seen that the rates are further reduced by almost an order of magnitude. Clearly, some additional measurements are desirable, preferably under different experimental conditions, in order to determine which rates may most reliably be used. Such measurements are reported in this Note.

Whereas the previous measurements were made behind the primary shock in a hydrogen-helium mixture in an arc driven shock tube, those reported here were conducted in the flow of a hydrogen-neon mixture over an inclined flat plate in the test section of a free piston, nonreflected shock tunnel. The mixture ratio used was 0.6 H_2 – 0.4 Ne.

Test Apparatus and Instrumentation

The shock tunnel was operated with a double diaphragm shock tube, 75 mm in diameter. Helium driver gas was compressed from an initial pressure of 47 kNm^{-2} to the main diaphragm rupture pressure of 75 MNm^{-2} and used to drive a shock wave through an intermediate shock tube, containing helium at 27.5 kNm^{-2}. This shock tube was 3.9 m long and was terminated by an 0.15-mm-thick mylar diaphragm, which was ruptured upon arrival of the shock wave to initiate flow in a test shock tube 4.4 m long.

An axisymmetric contoured nozzle was located at the downstream end of the test shock tube, with an inlet diameter of 37 mm and an exit diameter of 132 mm. The prior steady flow technique was used to insure rapid starting of the nozzle test flow. This technique is explained in Refs. 4 and 5, and a description of mechanical features associated with its use in the present situation is given in Ref. 5. The period of steady flow in the nozzle was determined by using bar gages to monitor the test section pitot pressure. These showed an initial overshoot in pressure, arising from the starting shock system, followed by a period of essentially constant pressure which lasted for approximately 20 μs before arrival of the contact surface. Bar gage pitot surveys in the test section showed that the nozzle produced a flow which was essentially uniform over at least a 100 mm test core, and was parallel to within an accuracy of ± 2 deg.

The test shock tube was filled with the hydrogen-neon mixture at a pressure of 0.66 kNm^{-2}. The neon supplied was specified as containing up to 10% helium, with other impurities less than 10 p.p.m. and the hydrogen as containing up to 0.04% of oxygen and nitrogen, with other impurities less than 100 p.p.m. Calculations indicate that these impurities would not affect the measurements, even if they were fully singly ionized before hydrogen ionization commenced. The test shock tube leak rate was less than 10^{-3} Torr min^{-1}, and it was evacuated and flushed with the test gas before filling for each shot.

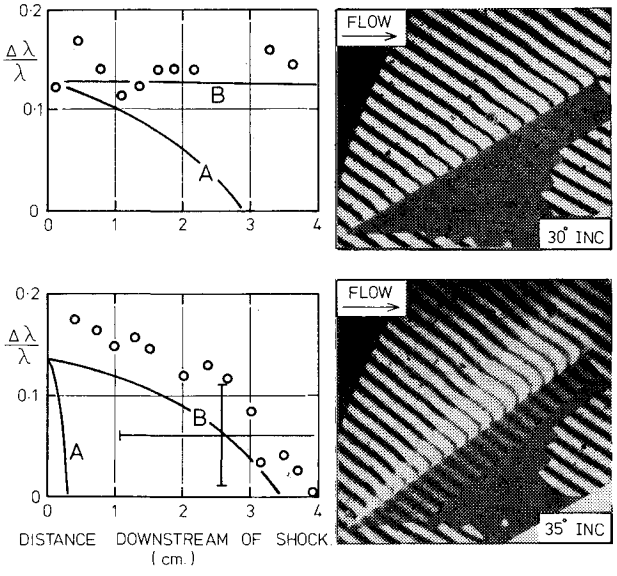

Fig. 1 Relaxation downstream of oblique shock in test section ($0.6H_2$ – 0.4 Ne, Primary shock speed = 11.4 km s^{-1}).

Shock speeds were measured using thermocouples, and radiation detectors, together with the test section bar gage. Shock attenuation was 6%/m in the test shock tube.

The flat plate model had a sharp leading edge, a chord of 50 mm, a span of 100 mm, and was mounted with the leading edge within 5 mm of the axis of the nozzle. The flow over the plate was viewed with a Mach-Zehnder interferometer, with its optical axis normal to the direction of the flow, and parallel to the surface of the plate. A nitrogen laser pumped dye laser light source was used, with peak emission at 590 nm, and a pulse duration of 5 ns. A filter limited the optical bandwidth received at the camera to 10 nm. The light source was triggered toward the end of the period of steady flow. Consideration of model flow transit times indicated that this allowed sufficient time to establish steady flow over the model, and this was confirmed by other experiments.

Flow conditions in the test section were calculated for a one-dimensional, steady nozzle expansion from the equilibrium conditions following the primary shock.[6] The shock speed at a point 0.6 m upstream of the nozzle entrance was used. For the results presented in Fig. 1 this yielded a test section flow with negligible ionization, a hydrogen dissociation fraction of 0.95, and a flow velocity of 12.8 km s^{-1}, at a frozen flow Mach number of 6.5 These values were independent of the choice of ionization rates in Table 1. The test section pitot pressure was 110 ± 8 kNm^{-2}, and was obtained from the shock speed by using a previous bar gage pitot survey of the test section flow.

Results and Calculations

Interferograms obtained at plate incidences of 30 and 35 deg are presented in Fig. 1. Luminosity patterns on the interferograms should be ignored, as they are likely to represent starting processes. Results at higher incidences were not used, as leading-edge detachment of the bow shock wave made analysis difficult. The flow interferograms were analyzed by taking an interferogram of the field of view before each shot, and using this to print a transparent mask which, when compared with the flow interferogram, allowed accurate measurement of fringe shift. The resultant measurements are presented in Fig. 1 adjacent to their respective interferograms. It can be seen that at 30 deg the fringe shift is constant downstream of the leading edge, whereas at 35 deg electron production by ionization causes the fringe shift to reduce with increasing distance from the shock.

The effect of the rate constants of Table 1 on this process was computed for constant pressure flow over the plate, since estimates had shown that the pressure changes induced by ionization were negligible. The relaxation process began with the conditions immediately downstream of the leading edge shock, which were calculated from the measured shock angle. This yielded a flow deflection which corresponded with the plate incidence to within 1 deg, thereby confirming the essentially monatomic nature of the test gas upstream of the shock. The model described by Leibowitz[3] was used for the ionization kinetics. This involved a separate electron and heavy particle temperature, with the electron temperature determined by assuming that energy is used by the electrons for ionization at the same rate as it is received from elastic collisions, i.e., a "steady-state" approximation. Due to the larger mass of the atom, and the lower collision cross section with electrons,[7] the energy received by elastic collisions with neon atoms was accounted negligible compared with that received from hydrogen atoms. The cross section for excitation of hydrogen by neon was taken to be the same as for helium, implying that the rate constants of Table 1 for a helium collision partner could be used for a neon collision partner. The temperatures involved were sufficiently low that excitation of neon could be neglected.

Fringe shifts were calculated according to the relation[8] $\Delta\lambda/\lambda = (4.20\, n_H + 2.49\, n_N)10^{-30}\, L/\lambda - 4.5\times 10^{-20}\, n_e L\lambda - \zeta$, where n_H, n_N and n_e, respectively, are the number of hydrogen atoms, neon atoms, and electrons per cubic meter, λ is the light wavelength, L is the span of the plate, and $\zeta = 0.05$ is the freestream fringe shift. End effects on the model span were estimated to contribute less than 5% to the fringe shift, and were ignored.

Results of the calculations are compared with experiment in Fig. 1. It can be seen that, at both angles of incidence, only the B set of rates is consistent with the observed results. The horizontal error bar shown for the B set at 35 deg incidence corresponds to an uncertainty of $\pm .3$ km s^{-1} in the shock speed, together with ± 2 deg in the shock angle, while the vertical error bar corresponds to an uncertainty of ± 0.05 in the measured fringe shift. These uncertainties allow the rate constants to be in error by a factor of 3. It should be noted that the immediate post shock temperatures of 16000 K or less, which were obtained in these experiments, were characteristic of those obtained in the experiments which yielded set A.[3] The present agreement with set B, which were obtained with somewhat higher temperatures, indicates that the rate constants of set B are satisfactory for analysis of flowfields, at least up to temperatures at which the dissociation time ceases to be short compared with the ionization time.

Acknowledgments

The experiments were performed in the Physics Department, at the Australian National University, Canberra. The assistance of H. G. Hornung, R.J. Sandeman, and R. French in setting up the experiment is gratefully acknowledged, together with that of V. Adams in running the shock tunnel. Financial support was provided by the Australian Research Grants Committee.

References

[1] Leibowitz, L.P. and Kuo, T-J, "Ionizational Nonequilibrium Heating during Outer Planetary Entries," *AIAA Journal,* Vol. 14, 1976, pp. 1324-1329.

[2] Belozerov, A.N. and Measures, R.M., "The Initial Ionization of Hydrogen in a Strong Shock Wave," *Journal of Fluid Mechanics,* Vol. 36, 1969, pp. 695-720.

[3] Leibowitz, L.P., "Measurements of the Structure of an Ionizing Shock Wave in a Hydrogen-Helium Mixture," *The Physics of Fluids,* Vol. 16, 1973, pp. 59-68.

[4] Stalker, R.J. and Mudford, N.R., "Starting Process in the Nozzle of a Nonreflected Shock Tunnel," *AIAA Journal,* Vol. 11, 1973, pp. 265-266.

[5] Mudford, N.R. and Stalker, R.J., "The Production of Pulsed Nozzle Flows in a Shock Tube," AIAA Paper 76-357, San Diego, Calif.

[6] Mudford, N.R., "Pulsed Nozzle Flows in a Shock Tube," Ph.D. Thesis, Australian National University, Canberra, 1976.

[7] Phelps, A.V., Fundingsland, O.T., and Brown, S.C., "Microwave Determination of the Probability of Collision of Slow Electrons in Gases," *Physical Review,* Vol. 84, 1951, pp. 559-562.

[8] Allen, C.W., *Astrophysical Quantities,* University of London, Athlone Press, 1963, p. 86.